https://doi.org/10.5194/egusphere-2025-2405
Preprint. Discussion started: 25 June 2025

Long-term pig manure application increases soil organic carbon through aggregate protection and Fe-carbon associations in a subtropical Red soil (Udic Ferralsols)

Hui Rong[a,b], Zhangliu Du[c], Weida Gao[a], Lixiao Ma[d], Xinhua Peng[e], Yuji Jiang[f], Demin Yan[g], Hu Zhou[a,*]

[a] *Key Laboratory of Arable Land Conservation (North China), Ministry of Agriculture, College of Land Science and Technology, China Agricultural University, Beijing, China*

[b] *State Key Laboratory of Soil and Sustainable Agriculture, Institute of Soil Sciences, Chinese Academy of Sciences, 71 East Beijing Road, Nanjing 210008, China*

[c] *College of Resources and Environmental Sciences, China Agricultural University, Beijing 100193, China*

[d] *State Key Laboratory of Vegetation and Environmental Change, Institute of Botany, Chinses Academy of Sciences, Beijing 100093, China.*

[e] *Institute of Agricultural Resources and Regional Planning, Chinese Academy of Agricultural Sciences, Beijing 100081, China*

[f] *College of Resources and Environment, Fijian Agriculture and Forest University, Fuzhou, 350002, China.*

[g] *Forest Fire Research Center, Nanjing Forest Police College, Nanjing 210023, China.*

Correspondence: Hu Zhou (zhouhu@cau.edu.cn)

Abstract

Manure is known to improve soil organic carbon (SOC) in Fe-rich red soils, while the underlying stabilization mechanisms remain poorly understood. In this study, four treatments were selected: (1) no amendment (Control), (2) low manure (LM, 150 kg N ha^{-1} yr^{-1}), (3) high manure (HM, 600 kg N ha^{-1} yr^{-1}), (4) high manure with lime (HML, 600 kg N ha^{-1} yr^{-1} plus 3000 kg Ca $(OH)_2$ ha^{-1} $3yr^{-1}$). The quantity and quality of topsoil (0-20 cm) organic carbon were investigated by physical fractionation, ^{13}C-nuclear magnetic resonance (NMR) spectroscopy and thermogravimetry (TG) analysis. Manure application increased total SOC by 65.1%-126.7% (primarily in the particulate organic matter (POM) fraction), while the mineral-associated organic matter fraction (MAOM), despite its higher C content (4.18-7.09 g C kg^{-1}), contributed less (65.4%-71.0%) compared to the control (82.4%). POM C was stabilized via hierarchical aggregation: fresh manure inputs acted as binding nuclei, increasing macroaggregates (>0.25 mm) while reducing microaggregates (0.05–0.25

* Corresponding author:
Tel number: +86 13405876151
E-mail address: zhouhu@cau.edu.cn

https://doi.org/10.5194/egusphere-2025-2405
Preprint. Discussion started: 25 June 2025

mm), physically isolating labile C from microbial decomposition. Concurrently, manure amendments triggered Fe-mediated chemical stabilization. Elevated pH (4.8 to 5.4-7.1) enhanced non-crystalline Fe oxide (Fe_o) content (+25.4%), which positively correlated with MAOM C (R^2 = 0.56, $P < 0.05$). Despite a chemical composition shift toward aliphaticity and reduced aromaticity, thermally stable organic matters increased by 8%–12%, revealing critical role of Fe_o (aggregates were destroyed before TG analysis) in offsetting inherent molecular lability. Overall, this study establishes a dual SOC stabilization framework for subtropical red soils, highlighting physical protection through aggregation processes and chemical protection via Fe-carbon associations.

Keywords: Particulate organic matter; Mineral-associated organic matter; Nuclear magnetic resonance; Thermogravimetry analysis

1. Introduction

Soil organic carbon (SOC), the largest carbon reservoir in the terrestrial ecosystems, plays critical roles in climate mitigation and soil multifunctionality (Amelung et al., 2020; Lal, 2004). In tropical and subtropical South China, red soils (Udic Ferralsols, according to Chinese Soil Taxonomy) are characterized by inherently low SOC content due to intense weathering and rapid mineralization (Yan et al., 2013; Zhang et al., 2013). While manure application has been widely adopted to enhance SOC in these soils (Bai et al., 2023; Nichitha et al., 2023; Zhang et al., 2023), the mechanisms governing SOC stabilization remain elusive. Discrepancies continue regarding whether manure predominately increases SOC through chemical recalcitrance, physical protection (by aggregation process), or organo-mineral interactions—given the iron-rich mineralogy of red soils and their pH-dependent reactivity (Kleber et al., 2021; Six et al., 2002; Song et al., 2022).

Existing studies present conflicting evidence on SOC stabilization pathways. For instance, Mustafa et al. (2021) reported increased aromatic C (chemically recalcitrant) with manure application, whereas Yan et al. (2013) observed preferential accumulation of labile O-alkyl C. This paradox highlights uncertainties in how manure inputs alter SOC composition. Fe oxides contribute a lot to SOC stabilization in red soils (Zhang et al., 2013). These reactive Fe phases can form stable covalent bonds between their surface hydroxyls and organic functional groups, protecting SOC from microbial decomposition (Ruiz et al., 2024). In comparison with crystalline Fe oxides (Fe_d), non-

https://doi.org/10.5194/egusphere-2025-2405
Preprint. Discussion started: 25 June 2025

crystalline Fe oxides (Fe_o) exhibit organic matter adsorption capacity primarily attributed to their larger specific surface area (Zhang et al., 2013). The ratio of Fe_d and Fe_o is dynamically regulated by pH, which can be intentionally manipulated through manure application (Liu et al., 2020; Wang et al., 2023). The long-term impacts of manure-induced pH shifts on Fe oxide speciation and related organic carbon sequestration are still not well understood, despite the known connection between pH-driven Fe oxide transformation and organic matter stabilization. Additionally, previous studies often isolated chemical recalcitrance, physical protection (via aggregation), or organo-mineral interactions separately, thereby neglecting integrative assessments among these pathways. To address this knowledge gap, an integrative approach combining physical fractionation, molecular characterization, and thermal stability analysis is essential for elucidating the coupled effects of manure on SOC quantity and quality.

Physically separating soil organic matter into mineral-associated organic matter (MAOM) and particulate organic matter (POM) fractions helps predicting SOC dynamics better, and clarifying SOC stabilization mechanisms, with POM C physically protected in aggregated and MAOM C chemically protected via organo-mineral bonding (Chenu et al., 2019; Lavallee et al., 2019; Poeplau et al., 2018). While physical fractionation effectively isolates operationally defined pools (Poeplau et al., 2018), it fails to reveal chemical heterogeneity of SOC (Cotrufo et al., 2019; Lavallee et al., 2019). Solid-state ^{13}C nuclear magnetic resonance (NMR) spectroscopy addresses this gap by quantifying carbon functional groups (alkyl, O-alkyl, aromatic C), yet its reliance on hydrofluoric acid (HF) pretreatment risks altering native organo-mineral interactions (Kögel-Knabner, 1997). Conversely, thermogravimetry (TG) provides rapid assessment of SOC thermal stability without requiring pretreatment (Gao et al., 2015).

We hypothesized that: 1) Manure application enhance MAOM C formation by increasing non-crystalline Fe oxides (Fe_o), induced by elevated pH; 2) The physical protection was strengthened after manure application due to the soil aggregation process, which triggered labile SOC protection; 3) The application of pig manure strengthened the recalcitrance of SOC, thus improved thermal stability. The specific objectives of this studies were: 1) to evaluate the changes of Fe oxides and its effect on MAOM formation; 2) to explore how soil aggregation affected POM formation; 3) to evaluate the effect of manure application on SOC composition and stability.

https://doi.org/10.5194/egusphere-2025-2405
Preprint. Discussion started: 25 June 2025

2. Materials and methods

2.1. Site description and experimental design

The long-term field experiment is located at Yingtan National Agroecosystem Field Experiment Station of the Chinese Academy of Sciences (28°15′20″N, 116°55′30″E) in Jiangxi Province, China. The site has a typically subtropical humid monsoon climate with a mean annual temperature of 17.6℃ and precipitation of 1795 mm (Jiang et al., 2018). The soil is derived from Quaternary red clay, and is classified as Udic Ferralsols according to Chinese Soil Taxonomy. The soil contains 36.3% clay, 45.2% silt and 21.2% sand.

The field experiment was initiated in 2002. Four treatments were compared: (1) no manure amendment (Control), (2) low pig manure with 150 kg N ha^{-1} a^{-1} (LM), (3) high pig manure with 600 kg N ha^{-1} a^{-1} (HM), and (4) high pig manure with 600 kg N ha^{-1} a^{-1} and lime (HML). The four treatments received solely pig manure as the nitrogen source, with no synthetic fertilizers applied. The pig manure, collected from nearby pig farms, contained an average total carbon of 386.5 g kg^{-1}, total nitrogen of 36.2 g kg^{-1} and total phosphorus of 21.6 g kg^{-1} on a dry matter basis. The annual amount of pig manure applied to each treatment was calculated based on its nitrogen content. Since all aboveground residues (stalks and leaves) and manually recoverable roots were completely removed from the field after harvest, the total carbon inputs to the soil were derived exclusively from pig manure**.** This resulted in average annual carbon inputs of 1.6 and 6.4 Mg C ha^{-1} for the LM and HM treatments, respectively (see Supplementary Material for calculation details). The field experiment was set up following a completely randomized design, with each treatment has three replicate plots. Each plot has a size of 2 m × 2 m. Lime was applied at 3 000 kg $Ca(OH)_2$ ha^{-1} $(3a)^{-1}$ for the HML treatment. The field was planted with corn (*Zea mays L.*) monoculture annually from April to July. All the management measures, including sowing, harvesting and weeding, were manually operated.

2.2 Sampling

Sampling was conducted in July 2019, after the harvest of corn. Triplicate topsoil samples (0-20 cm) were randomly collected with a shovel from each plot and composited together to form one bulk sample. The soil samples were air-dried at room temperatureand were gently crushed with a

https://doi.org/10.5194/egusphere-2025-2405
Preprint. Discussion started: 25 June 2025

rubber mallet to pass through an 8-mm sieve, preserving aggregates >8mm for further analysis. Visible plant residues, roots and stones were removed (Soil Survey Staff, 2011).

2.3 Soil properties measurements

SOC and Total nitrogen (TN) were determined by an elemental analyzer (Vario MACRO, Elementar, Germany). Soil pH was measured using a glass electrode (PHS-3D, SANXIN, China) with soil: deionized water ratio of 1: 2.5. Crystalline (Fe_d) and non-crystalline Fe oxides (Fe_o) were extracted by DCB (Dithionite-citrate-bicarbonate) and oxalate, respectively (Yan et al., 2013), and then were determined by graphite furnace atomic absorption spectrometry (GFAAS) (PinAAcle 900T, PerkinElmer, America). Water stability of aggregates was tested using the fast-wetting method following Le Bissonnais (1996). Aggregate stability was expressed as mean weight diameter (MWD). Detailed experimental processes and calculation can be found in Zhou et al. (2019).

2.4. Physical fractionation

Soil was fractionated into MAOM (<53 μm) and POM (>53 μm) fraction following Cambardella and Elliott (1992) and Cotrofu et al. (2019). Briefly, 10 g sieved samples (<2 mm) were completely dispersed in dilute sodium hexametaphosphate ($(NaPO_3)_6$, 0.5%) at a soil: solution ratio of 1:4 by shaking for 18 h (25°C, 180 r min^{-1}). After dispersing, soil slurry was passed through a 53 μm sieve and rinsed several times with deionized water. The fraction passing through the sieve was collected as MAOM fraction, and that remaining on the sieve was collected as POM fraction. Both fractions were centrifuged and the solution was decanted, and then the remaining material was oven-dried to constant weights at 60°C. SOC concentration of each fraction was measured using the wet oxidation method. Dried mass proportions of each fraction (g fraction g^{-1} soil) were calculated as follows:

$$f_M = m_M / m_{bulk} \quad (1)$$

$$f_P = m_P / m_{bulk} \quad (2)$$

where f_M and f_P were the dried mass proportions of MAOM and POM fraction (g fraction g^{-1} bulk soil), respectively; m_M and m_P (g)were the dried masses of MAOM and POM fractions; m_{bulk} (g) was the dried mass of bulk soil.

SOC in the MAOM and POM fractions were called as MAOM C and POM C, respectively in this paper. MAOM C and POM C were calculated by multiplying the dried mass proportions of each fraction (g fraction g^{-1} soil) by the respective SOC concentrations (g C kg^{-1} fraction) as follows

https://doi.org/10.5194/egusphere-2025-2405
Preprint. Discussion started: 25 June 2025

(Garten and Wullschleger, 2000; Lian et al., 2015):

$$\text{MAOM C} = f_M \times \text{SOC}_M \quad (3)$$

$$\text{POM C} = f_P \times \text{SOC}_P \quad (4)$$

where f_M and f_P were calculated by Equation (1) and Equation (2); SOC_M and SOC_P were the SOC concentrations in the MAOM and POM fraction (g C kg^{-1} fraction), respectively.

The contributions of MAOM C and POM C to total SOC (%) was calculated as:

$$\text{Contribution of MAOM C (\%)} = \text{MAOM C} / \text{Total SOC} \times 100 \quad (5)$$

$$\text{Contribution of POM C (\%)} = \text{POM C} / \text{Total SOC} \times 100 \quad (6)$$

where MAOM C and POM C were derived from Equations (3) and (4), respectively; total SOC was the content of SOC in the bulk soil.

2.5. SOC chemical composition and chemical stability

SOC chemical composition was analyzed with a solid-state cross-polarization magic angle spinning (CPMAS) ^{13}C nuclear magnetic resonance (NMR) spectroscopy. Prior to NMR analysis, <2 mm air-dried soils were pretreated with hydrofluoric acid (HF) to remove paramagnetic Fe^{3+} (iron oxides) following Gao et al. (2021). Firstly, 20 g soil was mixed with 100 mL 10% (w/w) HF solution in a polyethylene bottle and then shaken for 0.5 h per day for three days. Afterwards, the supernatant liquid was discarded and another 100 mL 10% HF solution was added again. The above procedures were repeated for 15 times. The residue was rinsed 10 times with deionized water until the pH was close to neutral. The remaining soil was freeze-dried and then ground in an agate mortar to pass through a 100-mesh sieve (0.149 mm) for further analysis. This fine grinding ensured homogeneous packing in the NMR rotor, minimizing signal heterogeneity (Simpson & Simpson, 2012).

Carbon functional groups were determined with the Bruker Ascend 500 MHz NMR spectrometer (Bruker BioSpin, Rheinstetten, Germany). Dry powdered samples were placed in a 4-mm sample rotor operating at a ^{13}C resonance frequency of 125.8 MHz. The NMR spectrometer run at a spinning rate of 5kHz, and 10500 scans were collected for each sample. The spectra were collected over an acquisition time of 12 ms and a recycle delay of 0.8 s. We assigned the obtained spectra to four different carbon functional groups, i.e., alkyl C (0-45 ppm), O-alkyl C (45-110 ppm), aromatic C (110-160 ppm) and carbonyl C (160-220 ppm) according to Kögel-Kanbner (1997). The relative

https://doi.org/10.5194/egusphere-2025-2405
Preprint. Discussion started: 25 June 2025

concentrations of the different functional groups were calculated as the percentage of their peak areas to the total aeras using MestReNova 14.0 software (Mestrelab Research, 2019, Spain). Indices used to evaluate SOC recalcitrance include: alkyl C/O-alkyl C, aromaticity, aromatic C/O-alkyl C, aliphatic C/aromatic C and aliphaticity (Baldock et al., 1997; Du et al., 2017). Aromaticity = aromatic C / (alkyl C + O-alkyl C + aromatic C); Aliphatic C = alkyl C + O-alkyl C; Aliphaticity = (alkyl C + O-alkyl C) / (alkyl C + O-alkyl C + aromatic C). The alkyl C/O-alkyl C ratio reflects the degree of microbial transformation, with higher values indicating advanced decomposition and accumulation of recalcitrant alkyl compounds (Baldock et al., 1997). The aromatic C/O-alkyl C ration aligns with the alkyl C/O-alkyl C ration in reflecting the degree of SOC decomposition, whereas the aliphatic C/aromatic C ratio presents a contrary perspective to them. Aromaticity is a chemical concept denoting the resistance to microbial degradation (Kögel-Knabner, 1997). Aliphaticity is used to quantify the proportion of labile aliphatic components relative to stable aromatic moieties.

2.6. Thermogravimetry analysis

TG analysis was performed using a Netzsch TG 209F1 (Netzsch-Gerätebau GmbH, Selb, Germany). Air-dried soil samples were first sieved through a 2-mm mesh, and then ground in a ball mill to pass through a 50 μm sieve. The grounded soil samples (5 ~ 10 mg) were placed in an Al_2O_3 crucible covered with an aluminum lid and were oxidized in an atmosphere of 20 mL min^{-1} of synthetic air (20% O_2 and 80% N_2) and 20 mL min^{-1} of N_2 as a protective gas. The temperature program included a heating rate of 10°C min^{-1} from 40°C up to 800°C. The sample mass percentage relative to the initial mass as a function of temperature was recorded simultaneously, and its first derivative (DTG) was calculated to represent the mass loss rate.

Three processes were detected in the temperature range of 40°C to 800°C: hygroscopic moisture evaporation, SOM decomposition and carbonate breaking down (Gao et al., 2015; Siewert, 2004). Based on the observed DTG curve, the weight loss between 180°C and 530°C, representing the temperature range during which SOM was decomposed, was defined as the total mass of SOM (Exo_{tot}). The mass loss between 180°C and 380°C was a consequence of thermally labile SOM oxidation (Exo_1) and that between 380°C and 530°C was caused by the combustion of more stable organic matter (Exo_2) (Gao et al., 2015; Volkov et al., 2020). We used two parameters, the ratio of

https://doi.org/10.5194/egusphere-2025-2405
Preprint. Discussion started: 25 June 2025

Exo_1 and Exo_{tot} (Exo_1/ Exo_{tot}) and the temperature at which half of the SOM was decomposed (TG-T_{50}), to characterize the thermal stability of SOM. Higher Exo_1/ Exo_{tot} and lower TG-T_{50} values indicate that the sample has more thermally labile or unstable SOM (Gao et al., 2015; Siewert, 2004).

2.7. Statistical analysis

Statistical analyses were carried out with R Studio software (R Development Core Team, version 4.1.2). One-way analysis of variance (ANOVA) was conducted to assess the effect of amendments on soil physico-chemical properties, SOC physical fractions, chemical composition and thermal indices. The independence of samples, normality of residues and homogeneity of variances were checked by Chisq, Shapiro-Wilk and Bartlett test, respectively. Fisher's least significant difference (LSD) method was used for the multiple comparisons of means with a 0.05 significance level. Linear regression analysis was conducted to investigate the correlations between SOC and iron oxides, soil aggregation. Principal component analysis (PCA) was performed to evaluate the relationship between the quantity and quality of SOC and factors related to chemical protection and physical protection. Pearson correlation analyses were performed to explore the relationships between chemical composition and thermal indices.

3. Results

3.1. Long-term pig manure application increased SOC, TN, pH, non-crystalline (Fe_o) and improved soil aggregation

Long-term manure amendment altered the soil physic-chemical properties (Table 1). Relative to Control, the LM, HM and HML treatments increased SOC concentration by 64.9%, 116.2% and 126.6%, respectively ($P < 0.05$), and increased TN concentration by 48.0%-108.2% ($P < 0.05$). The pH values were increased by 0.62-2.28 units after pig manure application ($P < 0.05$). Application of pig manure had no significant effect on crystalline iron oxides (Fe_d) content ($P > 0.05$), but the HM and HML treatments significantly increased non-crystalline iron oxides (Fe_o) by 25.4% ($P < 0.05$). Relative to Control, the HM and HML treatments significantly increased macroaggregates (>0.25 mm) content by 15.8% and 16.8%, respectively, and they increased MWD by 24.3% and 35.0%, respectively ($P < 0.05$). Microaggregates (0.05-0.25 mm) was decreased by 30.4% and 36.4%, respectively under the HM and HML treatments ($P < 0.05$).

3.2. Long-term pig manure application affected SOM physical fractions: MAOM and POM

https://doi.org/10.5194/egusphere-2025-2405
Preprint. Discussion started: 25 June 2025

The distribution of MAOM and POM fractions was significantly influenced by manure and lime amendments ($P < 0.05$, Table 2). Across all treatments, MAOM dominated the soil mass proportion (72.5%–75.1%), whereas POM mass proportion increased progressively from 16.6% in the control to 19.3%–19.4% under the HM and HML treatments.

Manure application improved SOC concentration in both fractions, with increase rates of 32.0%-66.8% and 208%-592% in the MAOM and POM fractions, respectively. Despite this, the contribution of MAOM to total SOC declined from 82.4% in the control to 65.5%–65.8% under the HM and HML treatments, while POM contribution increased nearly threefold (from 8.8% to 23.7%–26.0%). Lime addition (HML vs. HM) did not significantly alter mass proportions but further enhanced POM C concentration (+15.4%) and its SOC contribution (+9.7%).

3.3. Effect of long-term pig manure application on SOC chemical composition and recalcitrance

The solid-state ^{13}C NMR spectra showed different signal patterns for the different treatments (Fig. 1) and quantified the ratios of the different SOC functional groups shown in Table 3. Relative to Control, the HM and HML treatments significantly increased alkyl C by 4.6%-4.9% ($P < 0.05$), while the LM treatment showed no significant change ($P > 0.05$). The O-alkyl C was significantly increased by 5.5%, 2.6% and 2.2% under the LM, HM and HML treatments, respectively ($P < 0.05$). Aromatic C and carbonyl C were decreased by 12.4%-13.2% and 0.9%-8.7%, respectively, in the manured treatment ($P < 0.05$). While aromatic C was increased in the content after manure amend, its relative proportion was decreased by 12.4%-13.2% ($P < 0.05$).

Relative to Control, the LM treatment significantly decreased alkyl C/O-alkyl C ratio ($P < 0.05$), but the HM and HML treatments had no significant effect on the ratio ($P > 0.05$, Table3). The aromaticity was decreased by 14.4%, 12.9% and 13.2% under LM, HM and HML treatments, respectively ($P < 0.05$, Table3). Similarly, the aromatic C/O-alkyl C ratio was decreased by 14.7%-17.7% in the manured treatment ($P < 0.05$, Table3). In contrast, the aliphatic C/aromatic C ratio and aliphaticity were increased by 18.1%-20.7% and 2.44%-3.66% in the manured treatments, respectively ($P < 0.05$, Table3).

3.4. The effect of long-term pig manure application on SOC thermal stability

The shapes of TG and its first derivatives (DTG) curves showed distinct weight losses rate as temperature increased to above 100°C, in the order of HM>HML>LM>Control (Fig. 2). Relative to

https://doi.org/10.5194/egusphere-2025-2405
Preprint. Discussion started: 25 June 2025

Control treatment, pig manure application significantly increased the total mass losses in the range of 180℃ to 530℃ (Exo_{tot}) by 11.1%- 17.4% ($P < 0.05$, Table 4), and significantly increased the mass losses during 180-380℃ (Exo_1) and 380-530℃ (Exo_2) by 14.6%-26.5% and 7.8%-13.7%, respectively ($P < 0.05$, Table 4). The LM and HML treatments significantly increased the ratio of Exo_1/Exo_{tot} ($P < 0.05$), whereas the HM treatment had no significant effect ($P > 0.05$, Table 4). HM and HML treatments significantly decreased TG-T_{50} by 10.7-12.0 ℃ ($P < 0.05$), while LM treatments showed no significant difference compared to Control ($P > 0.05$, Table 4).

3.5. *Relationships between SOC and factors related to the mineral protection and physical protection of SOC*

Fig. 3 showed correlations between SOC and possible variables associated with the chemical protection and physical protection of SOC. SOC in the bulk soil was significantly positively correlated with MAOM C (R^2=0.97, Fig. 3A). While MAOM C showed no relationship with Fe_d (R^2=0.04, Fig. 3B), it was positively correlated with Fe_o (R^2=0.56, Fig. 3C). In addition, there was no correlation between MAOM C and the content of clay and silt (R^2=0.34, Fig.3D).

SOC in the bulk soil was significantly positively correlated with POM C (R^2=0.95, Fig. 3E). POM C was significantly associated with soil aggregation, evidenced by the positive correlation with macroaggregates (>0.25 mm) (R^2=0.78, Fig. 3F) and MWD (R^2=0.67, Fig. 3H), while negative correlation with microaggregates (<0.25 mm) (R^2=-0.71, Fig. 3G).

A PCA plot diagram (Fig. 4) revealed distinct associations between SOC quantity/quality and stabilization mechanisms. SOC vector aligned positively with POM C, macroaggregates and MWD, but inversely with microaggregates. Chemically, SOC covaried with MAOM C and Fe_o, yet formed an obtuse angle (>90°) with Fe_d. TG-T_{50} negatively associated with O-alkyl C and aliphaticity (angles > 90°), but positively linked to aromatic C and aromaticity (angles < 90°).

4. Discussion

4.1. POM C and physical protection

Long-term pig manure application caused an increase of SOC in the bulk soil, and the increase was mainly derived from continuous manure inputs (Gong et al., 2009). Although maize rhizodeposition (including root exudates and sloughed-off cells) (typically <10% of net primary productivity; Pausch and Kuzyakov, 2018) contributes to SOC during the growing season, its annual

https://doi.org/10.5194/egusphere-2025-2405
Preprint. Discussion started: 25 June 2025

carbon inputs is only 0.2-0.5 Mg C ha^{-1} yr^{-1} (Dennis et al., 2010). This contribution is negligible in comparison with manure inputs, which ranged from 1.6 to 6.4 Mg C ha^{-1} yr^{-1} in the LM and HM treatments, respectively. Furthermore, the rigorous removal of all harvest residues (stalks and recoverable roots) excluded aboveground and root biomass as a source of soil carbon deposition. Thus, the SOC increase in the LM/HM treatments (Table 1) can be predominately attributed to the exogenous organic C supplied by pig manure, and the HML treatment can be partly influenced by lime. Following microbial decomposition and transformation, the applied manure-C was progressively partitioned into distinct SOC pools.

Manure-derived carbon was preferentially allocated to the POM fraction rather than the MAOM fraction. The contribution of POM C to SOC increased nearly threefold (8.8% to 26.0%), while that of MAOM C decreased significantly from 82.4% in the Control to 65.4%–71.0% under manure application treatments (Table 2). The result was in line with Lan et al. (2022) and Li et al. (2018), who reported that increased manure substitution improved the POM C/MAOM C ratio, indicating manure was beneficial to the formation of POM C. Recent biomarker evidence demonstrated that plant-derived carbon contributes disproportionately to POM in comparison with MAOM fraction (Zou et al., 2023). Notably, ^{13}C isotopic tracing study revealed that 70%-87% of residue-derived SOC was accumulated in the POM fraction at two sites in the study of Mitchell et al. (2021). These results jointly validate that fresh organic inputs are distributed primarily in the POM fraction due to direct occlusion within macroaggregates before microbial processing. Therefore, POM C can be a good indicator of SOC dynamics under field management (Álvaro-Fuentes et al., 2021; Wu et al., 2023).

POM C was susceptible to decomposition due to its rapid dynamics, whereas it was simultaneously protected through physical occultation within soil aggregates. According to the classical hierarchical aggregation model (Six et al., 2000), organic carbon acts as a primary binding agent for microaggregates (<0.25mm) to form macroaggregates (>0.25mm), with POM serving as both a structural nucleus and a transient carbon reservoir (Six et al., 2000). In this study, macroaggregates were significantly increased, while microaggregates were significantly decreased after pig manure application (Table 1). These results implied that manure-derived carbon bound microaggregates to form macroaggregates, thus providing physical protection for SOC in the POM

https://doi.org/10.5194/egusphere-2025-2405
Preprint. Discussion started: 25 June 2025

fraction (Peng et al., 2023). The observed positive correlation between POM C and both macroaggregates and aggregate MWD (Fig.3; Fig.4) further verified the critical role of soil aggregation. However, the physical mechanisms by which POM facilitates this process (e.g., microbial mediation, hydrophobic interactions, or polysaccharide bridging) require further investigation. Experimental approaches such as isotopic labelling combined with micro-scale imaging (e.g., electron microscopy or X-ray computed tomography) can visualize the spatial distribution of POM within aggregates and quantify its role in aggregate formation. Future study should pay attention to these new technologies.

4.2. MAOM C and chemical protection

MAOM retained higher SOC concentrations (4.18-7.09 g C kg^{-1} bulk soil) irrespective of treatments, though its contribution to total SOC decreased after manure application (Table 2). MAOM C exhibited significantly longer mean residence time (MRT) compared to POM C, with reported turnover periods of 26-40 years versus 2.4-4.3 years, respectively (Benbi et al., 2014; Garten and Wullschleger, 2000). This fundamental difference originates from the unique stabilization mechanism of MAOM C through persistent organo-mineral associations (Lavallee et al., 2019). While clay minerals are widely recognized as key MAOM stabilizers (Hemingway et al., 2019; Liang et al., 2017), our study reveals a distinct iron oxide-dominated mechanism in these Fe-rich red soils. The strong correlation between MAOM C and non-crystalline Fe oxides (Fe_o, R^2=0.56; Figs. 3C, 4) contrasts with its weak relationship with clay + silt content (R^2=0.34; Fig. 3D), highlighting the pivotal role of Fe_o in this red soil. This iron-mediated stabilization likely stems from the exceptionally high specific surface area of Fe_o (~800 $m^2\ g^{-1}$ in ferrihydrite; Kleber et al., 2005) and its superior capacity to form stable organo-mineral complexes (Eusterhues et al., 2005; Lehmann and Kleber, 2015). The increased pH after manure application (Table 1) created conditions favoring Fe_o preservation (Vithana et al., 2015), with an increase of 25.4% in the content of Fe_o. The increased Fe_o content provided abundant reactive surfaces for MAOM formation. This pH-Fe_o-MAOM nexus establishes a self-reinforcing stabilization mechanism: manure-derived organic ligands interact with Fe_o to form stable complexes, simultaneously protecting both organic carbon and Fe_o from dissolution (Kleber et al., 2021).

https://doi.org/10.5194/egusphere-2025-2405
Preprint. Discussion started: 25 June 2025

The positive correlation between Fe_o and MAOM C (Fig. 3C) suggested that non-crystalline Fe oxides played a critical role in stabilizing SOC through organo-mineral interactions. However, while our data support the association between Fe_o and MAOM C, the underlying mechanisms (e.g., adsorption, co-precipitation, or ligand exchange) remain speculative due to the lack of direct molecular-scale evidence. Future studies employing advanced spectroscopic techniques (e.g., synchrotron-based X-ray absorption spectroscopy or NanoSIMS) could explicitly characterize the binding forms of Fe-organic complexes, thereby validating the causal relationship between Feo and MAOM formation.

4.3. Chemical composition and thermal stability

Input of new organic material could alter chemical composition of SOC and lead to the change of the molecule recalcitrance of SOC (Guo et al.,2019; Yan et al., 2013; Zhou et al., 2010; Zhang et al., 2013). In the current study, pig manure application increased the content of O-alkyl C, but declined that of aromatic C. Pig manure was rich in cellulose and lignin components, so the introduction of manure greatly increased O-alkyl C (Li et al., 2015). The considerable increase of O-alkyl C accounted for the decrease of the relative proportion of aromatic C and the decrease of aromaticity.

Long-term pig manure application strengthened SOC thermal stability by improving the content of thermally stable organic matters while it decreased TG-T_{50}. Thermal analysis suggested that manure amend significantly increased SOM content, evidenced by the increase of the mass losses during 180-530 ℃ (Exo_{tot}) (Table 4). The result was consistent with the change of SOC content measured by conventional method (Table 1), indicating TG technology was promising for measuring SOM content (Siewert, 2004; Tokarski et al., 2018). The decrease of TG-T_{50} reflected more easily decomposable SOC accumulated after manure application (Gao et al., 2015; Siewert, 2004). The result consisted with that in the NMR spectroscopy, where greater O-alkyl C and higher aliphaticity were found under manure treatments (Table 3). SOC with more O-alkyl C functional groups or higher aliphaticity was less likely to resist thermochemical degradation as revealed by the negative relationship between TG-T_{50} and aliphacity (Fig.4; Fig. 5) (Hou et al., 2019; Lehman and Kleber, 2015), thus leading to a decrease of TG-T_{50}. In this study, the thermally labile organic matters accounted for over half of the total organic matters, so the decrease of TG-T_{50} after manure

https://doi.org/10.5194/egusphere-2025-2405
Preprint. Discussion started: 25 June 2025

application was just a result of the increased thermally organic matters not the decrease of thermal stability. In contrast, thermal stability should be strengthened according to the increased thermally stable organic matters after manure application. Since soil structure was destroyed due to the ground process of soil samples before TG analysis, the increase of the thermally stable organic matters was ascribed to mineral protection, where the correlations between organic carbon and Fe oxides increased the thermally resistance of OC (Ruiz et al., 2023).

5. Conclusion

Manure application increased SOC quantity and improved its quality in Fe-rich red soils. SOC in the POM fraction exhibited the most pronounced response to manure inputs, while the majority of SOC was stored in the MAOM fraction. Furthermore, SOC was stabilized by distinct yet complementary mechanisms: physical protection via aggregation process, and chemical protection via Fe-organic associations induced by elevated pH. In addition, manure application increased thermally stable organic matters. However, to better understand inherent mechanisms, future work should focus on molecular-scale characterization of Fe-organic interactions using synchrotron techniques (e.g., Fe K-edge XANES/EXAFS), and in-situ visualization of POM-mediated aggregation through advanced imaging tools (e.g., SEM-TEM or μ-CT) coupled with ^{13}C-labelled manure to track POM dynamics within aggregates.

Acknowledgments

This work was financially supported by the NSFC-CAS Joint Fund Utilizing Large-scale Scientific Facilities (No. U1832188) and Chinese Universities Scientific Fund (2023RC047). We thank Yanyan Cai and Xing Xia for laboratory assistance.

Author contributions

HR conceived the experimental approach, took soil samples from the field, carried out the laboratory and data analyses, wrote the first draft of the manuscript, and contributed to subsequent drafts. ZLD helped analyze NMR spectrum and revise the manuscript. WDG contributed to interpretating TG data and revising the manuscript. LXM conducted the experiment of NMR. XHP helped design the experiment, and analyze data. YJJ contributed to the design of field experiment and the process of

https://doi.org/10.5194/egusphere-2025-2405
Preprint. Discussion started: 25 June 2025

taking soil samples. DMY contributed to the process of writing. HZ contributed to funding acquisition, conceiving the experimental approach, carrying out data interpretations, and the writing of all subsequent manuscript drafts.

Conflict of Interest

Hu Zhou is a member of the editorial board of SOIL.

References

Álvaro-Fuentes, J., Franco-Luesma, S., Lafuente, V., Sen, P., Usón, A., Cantero-Martínez, C., Arrúe, J.L., 2021. Stover management modifies soil organic carbon dynamics in the short-term under semiarid continuous maize. Soil Till. Res. 213. https://doi.org/10.1016/j.still.2021.105143.

Amelung, W., Bossio, D., de Vries, W., Kögel-Knabner, I., Lehmann, J., Amundson, R., Bol, R., Collins, C., Lal, R., Leifeld, J., Minasny, B., Pan, G., Paustian, K., Rumpel, C., Sanderman, J., van Groenigen, J.W., Mooney, S., van Wesemael, B., Wander, M., Chabbi, A., 2020. Towards a global-scale soil climate mitigation strategy. Nat. Commun. 11:5427. https://doi.org/10.1038/s41467-020-18887-7.

Baldock, J.A., Oades, J.M., Nelson, P.N., Skene, T.M., Golchin, A., Clarke, P., 1997. Assessing the extent of decomposition of natural organic materials using solid-state ^{13}C NMR spectroscopy. Soil Res. 35(5): 1061–1084. https://doi.org/10.1071/S97004.

Bai, X.X., Tang, J., Wang, W., Ma, J.M., Shi, J., Ren, W., 2023. Organic amendment effects on cropland soil organic carbon and its implications: A global synthesis. Catena. 231:107343. https://doi.org/10.1016/j.catena.2023.107343.

Benbi, D.K., Boparai, A.K., Brar, K., 2014. Decomposition of particulate organic matter is more sensitive to temperature than the mineral associated organic matter. Soil Biol. Biochem. 70, 183-192. https://doi.org/10.1016/j.soilbio.2013.12.032.

Cambardella, C.A., Elliott, E.J., 1992. Particulate soil organic-matter changes across a grassland cultivation sequence. Soil Sci. Soc. Am. J. 56(3), 777-783. https://doi.org/10.2136/sssaj1992.03615995005600030017x.

Chenu, C., Angers, D.A., Barre, P., Derrien, D., Arrouays, D., Balesdent, J., 2019. Increasing organic stocks in agricultural soils: Knowledge gaps and potential innovations. Soil Till. Res. 188, 41-52. https://doi.org/10.1016/j.still.2018.04.011.

Cotrufo, M.F., Ranalli, M.G., Haddix, M.L., Six, J., Lugato, E., 2019. Soil carbon storage informed by particulate and mineral-associated organic matter. Nature Geosci. 12(12), 989-996. https://doi.org/10.1038/s41561-019-0484-6.

Dennis, P.G., Miller, A.J., Hirsch, P.R., 2010. Are root exudates more important than other sources of rhizodeposits in structuring rhizosphere bacterial communities? FEMS Microbiol Ecol, 72, 313-327. https://doi.org/10.1111/j.1574-6941.2010.00860.x

Eusterhues, K., Rumpel, C., Kögel-Knabner, I., 2005. Organo-mineral association in sandy acid forest soils: importance of specific surface area, iron oxides and micropores. Eur. J Soil Sci. 56, 753-763. https://doi.org/10.1111/j.1365-2389.2005.00710.x.

Gao, Q.Q., Ma, L.X., Fang, Y.Y., Zhang, A.P., Li, G.C., Wang, J.J., Wu, D., Wu, W.L., Du, Z.L., 2021. Conservation

https://doi.org/10.5194/egusphere-2025-2405
Preprint. Discussion started: 25 June 2025

tillage for 17 years alters the molecular composition of organic matter in soil profile. Science of the Total Environment, 762, 143116.

Gao, W.D., Zhou, T.Z., Ren, T.S., 2015. Conversion from conventional to no tillage alters thermal stability of orga -nic matter in soil aggregates. Soil Sci. Soc. Am. J. 79(2), 585-594. https://doi.org/10.2136/sssaj2014.08.0334. https://doi.org/10.1016/j.scitotenv.2020.143116.

Garten, C.T., Wullschleger, S.D., 2000. Soil carbon dynamics beneath switchgrass as indicated by stable isotope analysis. J. Environ. Qual. 29(2), 645-653. https://doi.org/10.2134/jeq2000.00472425002900020036x.

Gong, W., Yan, X.Y., Wang, J.Y., Hu, T.X., Gong, Y.B., 2009. Long-term manure and fertilizer effects on soil organic matter fractions and microbes under a wheat–maize cropping system in northern China. Geoderma 149(3-4), 318-324. https://doi.org/10.1016/j.geoderma.2008.12.010.

Guo, Z.C., Zhang, J.B, Fan, J., Yang, X.Y., Yi, Y.L., Han, X.R., Wang, D.Z., Zhu, P., Peng, X.H., 2019. Does animal manure application improve soil aggregation? Insights from nine long-term fertilization experiments. Sci. Total Environ. 660, 1029-1037. https://doi.org/10.1016/j.scitotenv.2019.01.051.

Hemingway, J.D., Rothman, D.H., Grant, K.E., Rosengard, S.Z., Eglinton, T.I., Derry, L.A., Galy, V., 2019. Mineral protection regulates long-term preservation of natural organic carbon. Nature. 570, 2717-2726. https://doi.org/10.1038/s41586-019-1280-6.

Hou, Y.H., Chen, Y., Chen, X., He, K., Zhu, B., 2019. Changes in soil organic matter stability with depth in two alp -ine ecosystems on the Tibetan Plateau. Geoderma. 351, 153-162. https://doi.org/10.1016/j.geoderma.2019.05.034.

Jiang, Y.J., Zhou, H., Chen, L.J., Yuan, Y., Fang, H., Luan, L., Chen, Y., Wang, X.Y., Liu, M., Li, H.X., Peng, X.H., Sun, B., 2018. Nematodes and microorganisms interactively stimulate soil organic carbon turnover in the macroaggregates. Front Microbiol. 9, 2803. https://doi.org/10.3389/fmicb.2018.02803.

Kleber, M., Bourg, I.C., Coward, E.K., Hamsel, C.M., Myneni, S.C.B., Nunan., 2021. Dynamic interactions at the mineral-organic matter interface. Nat Rev Earth Environ 2, 402–421. https://doi.org/10.1038/s43017-021-00162-y.

Kleber, M., Mikutta, R., Torn, M.S., Jahn,R., 2005. Poorly crystalline mineral phases protect organic matter in acid subsoil horizons. Eur. J Soil Sci. 717-725. https://doi.org/10.1111/j.1365-2389.2005.00706.x.

Kleber, M., Bourg, I.C., Coward, E.K., Hansel, C.M., Myneni, S.C.B., Nunan, N., 2021. Dynamic interactions at the mineral–organic matter interface. Nat. Rev. Earth Env. 2(6), 402-421. https://doi.org/10.1038/s43017-021-00162-y.

Kögel-Knabner, I. 1997. ^{13}C and ^{15}N NMR spectroscopy as a tool in soil organic matter studies. Geoderma, 80, 243-270. https://doi.org/10.1016/S0016-7061(97)00055-4.

Lal, R., 2004. Soil carbon sequestration impacts on global climate change and food security. Science. 304(5677), 1623-1627. https://doi.org/10.1126/science.1097396.

Lan, Z.J., Shan, J., Huang, Y., Liu, X. M., Lv, Z.Z., Ji, J.H., Hou, H.Q., Xia, W.J., Liu, Y.R., 2022. Effects of long-term manure substitution regimes on soil organic carbon composition in a red paddy soil of southern China. Soil Till. Res. 221, 105395. https://doi.org/10.1016/j.still.2022.105395.

Lavallee, J.M., Soong, J.L., Cotrufo, M.F., 2019. Conceptualizing soil organic matter into particulate and mineral-associated forms to address global change in the 21st century. Glob Chang Biol. 26(1). https://doi.org/10.1111/gcb.14859.

Le, Bissonnais, Y., 1996. Aggregate stability and assessment of soil crustability and erodibility: I. Theory and methodology. Eur. J. Soil Sci. 47,425-437. https://doi.org/10.1111/j.1365-2389.1996.tb01843.x.

Lehmann, J., Kleber, M., 2015. The contentious nature of soil organic matter. Nature. 528(7580), 60-68. https://doi.org/10.1038/nature16069.

https://doi.org/10.5194/egusphere-2025-2405
Preprint. Discussion started: 25 June 2025

Li, J., Wen, Y., Li, X., Li, Y., Yang, X., Lin, Z., Song, Z, Cooper, J., Zhao, B., 2018. Soil labile organic carbon fractions and soil organic carbon stocks as affected by longterm organic and mineral fertilization regimes in the North China Plain. Soil Till. Res. 175, 281–290. https://doi.org/10.1016/j.still.2017.08.008.

Li, Z.Q., Zhao, B.Z., Wang, Q., Cao, X.Y., Zhang, J.B., 2015. Differences in chemical composition of soil organic carbon resulting from long-term fertilization strategies. PLoS One. 10(4), e0124359. https://doi.org/10.1371/journal.pone.0124359.

Lian, T.X., Wang, G.H., Yu, Z.H., Li, Y.S., Liu, X.B., Jin, J., 2015. Carbon input from ^{13}C-labelled soybean residues in particulate organic carbon fractions in a Mollisol. Biol. Fertil. Soils. 52(3), 331-339. https://doi.org/10.1007/s00374-015-1080-6.

Liang, C., Schimel, J.P., Jastrow, J.D., 2017. The importance of anabolism in microbial control over soil carbon storage. Nat. MicrobioL. 2, 1–6. https://doi.org/10.1038/nmicrobiol.2017.105.

Liu, S. B., Wang, J.Y., Pu, S.Y., Blagodatskaya, E., Kuzyakov, Y., Razavi, B. S., 2020. Impact of manure on soil biochemical properties: A global synthesis, Science of The Total Environment, 745, 141003, 0048-9697, https://doi.org/10.1016/j.scitotenv.2020.141003.

Mitchell, E., Scheer, C., Rowlings, D., Contrufo, F., Conant, R.T., Grace, P., 2021. Important constraints on soil organic carbon formation efficiency in subtropical and tropical grasslands. Glob. Change Bio. 27: 5383-5391. https://doi.org/10.1111/gcb.15807.

Mustafa A., Xu, H., Shah, S.A.A., Abrar, M.M., Maitlo, A.A., Kubar, K.A., Saeed, Q., Kamran, M., Naveed, M., Wang, B.R., Sun N., Xu, M.G., 2021. Long-term fertilization alters chemical composition and stability of aggregate-associated organic carbon in a Chinese red soil: evidence from aggregate fraction, C mineration, and ^{13}C NMR analyses. J. Soil Sediment. 21, 2483-2496. https://doi.org/10.1007/s11368-021-02944-9

Nichitha, C.V, Raghaven, S., Champa, B.V., Ganapathi, G., Sudarshan V., Nandita, S., Ravikumar, D., Nagaraja, MS., 2023. Role of organic manures on soil carbon stocks and soil enzyme activities in intensively managemend ginger production systems. International Journal of Recycling of Organic Waste in Agriculture, 1977064. 1579. https://doi.org/10.30486/IJROWA.2023.1977064.1579.

Pausch, J., Kuzyakov, Y., 2018. Carbon input by roots into the soil: Quantification of rhizodeposition from root to ecosystem cell. Global Change Biology, 24: 1-12. https://doi.org/10.1111/gcb.13850.

Peng, X.Y., Huang, Y., Duan, X.W., Yang, H., Liu J.X., 2023. Particulate and mineral-associated organic carbon fractions reveal the roles of soil aggregates under different land-use types in a karst faulted basin of China. Catena, 220(3):106721. https://doi.org/10.1016/j.catena.2022.106721.

Poeplau, C., Don, A., Six, J., Kaiser, M., Benbi, D., Chenu, C., Cotrufo, M.F., Derrien, D., Gioacchini, P., Grand, S., Gregorich, E., Griepentrog, M., Gunina, A., Haddix, M., Kuzyakov, Y., Kühnel, A., Macdonald, L.M., Soong, J., Trigalet, S., Vermeire, M.-L., Rovira, P., van Wesemael, B., Wiesmeier, M., Yeasmin, S., Yevdokimov, I., Nieder, R., 2018. Isolating organic carbon fractions with varying turnover rates in temperate agricultural soils – A comprehensive method comparison. Soil Biol. Biochem. 125(2), 10-26. https://doi.org/10.1016/j.soilbio.2018.06.025.

Ruiz, F., Rumpel, C., Dignac, M-F., Baudin, F., Ferreira, T. O., 2023. Combing thermal analyses and wet-chemical extractions to assess the stability of mixed-nature soil orgnaic matter. Soil Biol. Biochem. 187 (90), 109216. https://doi.org/10.1016/j.soilbio.2023.109216.

Ruiz, F., Bernardino, A. F., Queiroz, H. M., Otero, X. L., Rumpel, C., Ferreira, T. O., 2024. Iron's role in soil organic carbon (de)stabilization in mangroves under land use change. Nat. Commun. 10433.

Shi, R.Y., Liu, Z.D., Li, Y., Jiang, T.M., Xu, M.G., Li, J.Y., Xu, R.K., 2019. Mechanisms for increasing soil resistance to acidification by long-term manure application. Soil Till. Res. 185, 77-84. https://doi.org/10.1016/j.still.2018.09.004.

https://doi.org/10.5194/egusphere-2025-2405
Preprint. Discussion started: 25 June 2025

Siewert, C., 2004. Rapid screening of soil properties using thermogravimetry. Soil Sci. Soc. Am. J. 68(5), 1656-1661. https://doi.org/10.2136/sssaj2004.1656.

Simpson, M.J., and Simpson, A.J. 2012. The chemical ecology of soil organic matter molecular constituents. J. Chem. Ecol. 38(6): 768–784. https://doi.org/10.1007/s10886-012-0122-x.

Six, J., Elliot, E.T., Paustian, K., 2000. Soil macroaggregate turnover and microaggregate formation: a mechanism for C sequestratioin under no-tillage agriculture. Soil Biology & Biochemistry, 32, 2099-2103. https://doi.org/10.1016/S0038-0717(00)00179-6.

Six, J., Conant, R.T., Paul, E.A., Paustian, K., 2002. Stabilization mechanisms of soil organic matter: Implications for C-saturated of soils. Plant Soil. 241, 155-176. https://doi.org/10.1023/A:1016125726789.

Soil Survey Staff, 2011. Soil survey laboratory information manual. Soil survey investigations report No. 45, version 2.0. R. Burt (ed.). U.S. Department of Agriculture, Natural Resources Conservation Service. https://www.nrcs.usda.gov/sites/default/files/2022-10/SSIR45.pdf

Song, X.X., Wang, P., van Z, L., Bolan, N., Wang, H.L., Li, X.M., Cheng, K., Yang, Y., Wang, M., Liu, T.X., Li, F.B., 2022. Towards a better understanding of the role of Fe cycling in soil for carbon stabilization and degradation. Carbon Research. 1(1):5. https://doi.org/10.1007/s44246-022-00008-2.

Tokarski, D., Kučerík, J., Kalbitz, K., Demyan, M.S., Merbach, I., Barkusky, D., Ruehlmann, J., Siewert, C., 2018. Contribution of organic amendments to soil organic matter detected by thermogravimetry. J. Plant Nutr Soil Sc. 181(5), 664-674. https://doi.org/10.1002/jpln.201700537.

Vithana, C.L., Sullivan, L.A., Burton, E.D., Bush, R.T., 2015. Stability of schwertmannite and jarosite in an acidic landscape: Prolonged field incubation. Geoderma. 239-240, 47-57. https://doi.org/10.1016/j.geoderma.2014.09.022.

Volkov, D.S., Rogova, O.B., Proskurnin, M.A., Farkhodov, Y.R., Markeeva, L.B., 2020. Thermal stability of organic matter of typical chernozems under different land uses. Soil Till. Res. 197:104500. https://doi.org/10.1016/j.still.2019.104500.

Wang, S.B., Hu, K.L., Feng, P.Y., Wei, Q., Leghari, S.J., 2023. Determining the effects of organic manure substitution on soil pH in Chinese vegetable fields: a meta-analysis. J. Soil. Sediment. 23: 118-130. https://doi.org/10.1007/s11368-022-03330-9.

Wu, J.J., Zhang, H., Pan, Y.T., Cheng, X.L., Zhang, K.R., Liu G.H., 2023. Particulate organic carbon is more sensitive to nitrogen addition than mineral-associated organic carbon: A meta-analysis. Soil Till. Res. 232(16), 105770. https://doi.org/10.1016/j.still.2023.105770.

Yan, X., Zhou, H., Zhu, Q.H., Wang, X.F., Zhang, Y.Z., Yu, X.C., Peng, X.H., 2013. Carbon sequestration efficiency in paddy soil and upland soil under long-term fertilization in southern China. Soil Till. Res. 130, 42-51. https://doi.org/10.1016/j.still.2013.01.013.

Zhang, J.C., Zhang, L., Wang, P., Huang, Q.W., Yu, G.H., Li, D.C., Shen, Q.R., Ran, W., 2013. The role of non-crystalline Fe in the increase of SOC after long-term organic manure application to the red soil of southern China. Eur. J. Soil Sci. 64(6), 797-804. https://doi.org/10.1111/ejss.12104.

Zhang, B.Y., Dou, S., Guo, D., Guan, S., 2023. Straw inputs improve soil hydrophobicity and enhance organic carbon mineralization. Agronomy. 13(10), 2618. https://doi.org/10.3390/agronomy13102618.

Zhou, P., Pan, G.X., Spaccini, R., Piccolo, A., 2010. Molecular changes in particulate organic matter (POM) in a typical Chinese paddy soil under different long-term fertilizer treatments. Eur. J. Soil Sci. 61(2), 231-242. https://doi.org/10.1111/j.1365-2389.2009.01223.x.

Zhou, H., Fang H., Zhang, Q., Wang, Q., Chen, C., Mooney, S. J., Peng X.H., Du, Z. L., 2019. Biochar enhances soil hydraulic function but not soil aggregation in a sandy loam. Eur. J. Soil Sci. 70: 291-300. https://doi.org/10.1111/ejss.12732.

https://doi.org/10.5194/egusphere-2025-2405
Preprint. Discussion started: 25 June 2025

577 Zou, Z.C., Ma, L.X., Wang, X., Chen, R.R., Jones, D.L., Bol, R., Wu, D., Du, Z.L., 2023. Decadal application of
578 mineral fertilizers alters the molecular composition and origins of organic matter in particulate and
579 mineral-associated fractions. Soil Biol. Biochem. 182: 109042.
580 https://doi.org/10.1016/j.soilbio.2023.109042.

581

582

https://doi.org/10.5194/egusphere-2025-2405
Preprint. Discussion started: 25 June 2025

Table 1

Soil organic carbon (SOC), total nitrogen (TN), the ration of SOC to TN (SOC/TN), pH, crystalline iron oxides (Fe_d), non-crystalline iron oxides (Fe_o), aggregate size distribution and mean weight diameter (MWD) of water-stable aggregates under no manure (Control), low manure (LM), high manure (HM) and high manure plus lime (HML) treatments.

Treatments	SOC (g kg^{-1})	TN (g kg^{-1})	SOC/TN	pH	Fe_d (g kg^{-1})	Fe_o (g kg^{-1})	Aggregate size distribution (g g^{-1})			MWD (mm)
							>0.25 mm	0.05-0.25 mm	<0.05 mm	
Control	4.79c	0.67c	7.10b	4.80c	62.99a	1.81b	0.67c	0.28a	0.05a	0.98b
LM	7.91b	1.00b	7.94a	5.42c	59.98a	1.74b	0.71b	0.25a	0.04ab	1.09b
HM	10.37a	1.35a	7.69ab	6.11b	59.59a	2.25a	0.77a	0.19b	0.03b	1.22a
HML	10.86a	1.40a	7.76ab	7.08a	62.22a	2.29a	0.78a	0.18b	0.04ab	1.32a

Values are the means (n=3). Different lowercase letters after values in the same row indicate a significant difference among four manure treatments ($P < 0.05$).

Table 2

Mass proportion, SOC concentration and contribution of the mineral-associated organic matter (MAOM) (<53 μm) fraction, particulate organic matter (POM) (>53 μm) fraction under no manure (Control), low manure (LM), high manure (HM) and high manure plus lime (HML) treatments.

Treatments	Mass proportion (%)		SOC concentration (g C kg^{-1} soil)		Contribution to total SOC/%	
	MAOM	POM	MAOM	POM	MAOM	POM
Control	74.3a	16.6b	4.18c	0.44c	82.4a	8.8c
LM	75.1a	17.2ab	5.61b	1.26b	71.0b	15.9b
HM	73.9a	19.4a	6.81a	2.46a	65.8b	23.7a
HML	72.5a	19.3a	7.09a	2.84a	65.4b	26.0a

Values are the means (n=3). Different lowercase letters after values in the same row indicate a significant difference among four manure treatments ($P < 0.05$). Calculations follow the methodology described in Section 2.4.

https://doi.org/10.5194/egusphere-2025-2405
Preprint. Discussion started: 25 June 2025

Table 3

The contents of various C functional groups in CPMAS-^{13}C-NMR spectra under no manure (Control), low manure (LM), high manure (HM) and high manure plus lime (HML) treatments. Alkyl (0-45 ppm); O-alkyl C (45-110 ppm); aromatic C (110-160 ppm) and carbonyl C (160-220 ppm).

Treatments	alkyl C (%)	O-alkyl C (%)	aromatic C (%)	carbonyl C (%)	alkyl C/ O-alkyl C	aromaticity (%)	aromatic C/O-alkyl C	aliphatic C/ aromatic C	aliphaticity (%)
Control	25.4b	44.9c	15.3a	14.4a	0.57a	17.9a	0.34a	4.58b	82.1b
LM	26.2ab	47.4a	13.3b	13.1b	0.55b	15.3b	0.28b	5.53a	84.7a
HM	26.6a	46.1b	13.4b	13.9ab	0.58a	15.6b	0.29b	5.41a	84.4a
HML	26.5a	45.9b	13.3b	14.3a	0.58a	15.6b	0.29b	5.43a	84.4a

Values are the means (n=3). Different lowercase letters after values in the same row indicate a significant difference among four manure treatments ($P < 0.05$). Aromaticity = aromatic C/ (alkyl C + O-alkyl C + aromatic C); aliphatic C = (alkyl C + O-alkyl C); aliphaticity = (alkyl C + O-alkyl C) / (alkyl C + O-alkyl C + aromatic C).

Table 4

The mass losses during specific temperature ranges under no manure (Control), low manure (LM), high manure (HM) and high manure plus lime (HML) treatments. Exo_1 represents thermally labile soil organic matter (SOM); Exo_2 represents thermally stable SOM; Exo_{tot} represents total SOM. TG-T_{50} indicates the temperature at which half of the total SOM is lost.

Treatments	Exo_1 (180~380℃) (%)	Exo_2 (380~530℃) (%)	Exo_{tot} (180~530℃) (%)	Exo_1/Exo_{tot}	TG-T_{50} (℃)
Control	2.28c	2.36b	4.64b	0.49b	381a
LM	2.62b	2.54a	5.16a	0.51a	376ab
HM	2.69ab	2.68a	5.37a	0.50b	369b
HML	2.89a	2.56a	5.45a	0.53a	371b

Values are the means (n=3). Different lowercase letters after values in the same row indicate a significant difference among four manure treatments ($P < 0.05$).

https://doi.org/10.5194/egusphere-2025-2405
Preprint. Discussion started: 25 June 2025

Figure legends

Fig. 1 CPMAS-^{13}C-NMR spectra under no manure (Control), low manure (LM), high manure (HM) and high manure plus lime (HML) treatments. Alkyl (0-45 ppm); O-alkyl C (45-110 ppm); aromatic C (110-160 ppm) and carbonyl C (160-220 ppm)

Fig. 2 Thermogravimetry (TG) curves (a) and corresponding derivative thermogravimetry (DTG) curves (b) of soil organic matter (SOM) under no manure (Control), low manure (LM), high manure (HM) and high manure plus lime (HML) treatments

Fig. 3 The relationships between SOC and variables related to the chemical protection and physical protection

Fig. 4 Biplots of the principal component analysis (PCA) between the quantity and quality of SOC and variables related to chemical protection, physical protection across four manure application treatments (CK, Control; LM, low manure; HM, high manure; and HML, high manure plus lime)

Fig. 5 The relationships between SOC quantity, chemical recalcitrance and thermal stability

https://doi.org/10.5194/egusphere-2025-2405
Preprint. Discussion started: 25 June 2025

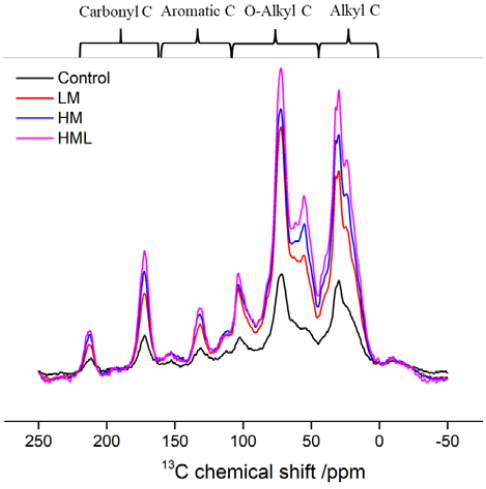

Fig.1 CPMAS-^{13}C-NMR spectra under no manure (Control), low manure (LM), high manure (HM) and high manure plus lime (HML) treatments. Alkyl (0-45 ppm); O-alkyl C (45-110 ppm); aromatic C (110-160 ppm) and carbonyl C (160-220 ppm)

https://doi.org/10.5194/egusphere-2025-2405
Preprint. Discussion started: 25 June 2025

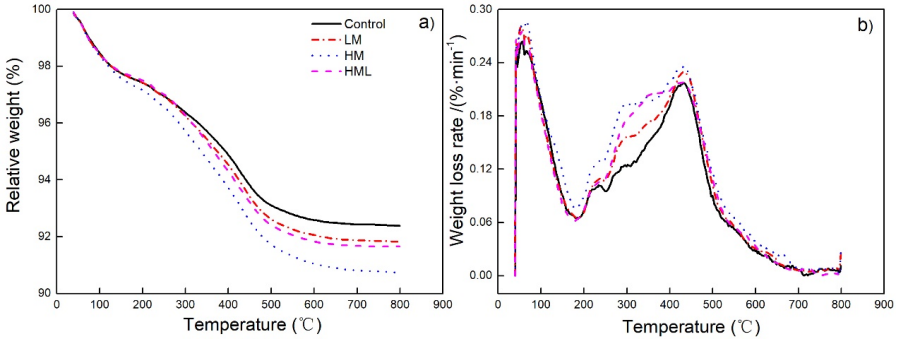

644

645 **Fig. 2** Thermogravimetry (TG) curves (a) and corresponding derivative thermogravimetry (DTG) curves (b) of soil
646 organic matter (SOM) under no manure (Control), low manure (LM), high manure (HM) and high manure plus
647 lime (HML) treatments

648

https://doi.org/10.5194/egusphere-2025-2405
Preprint. Discussion started: 25 June 2025

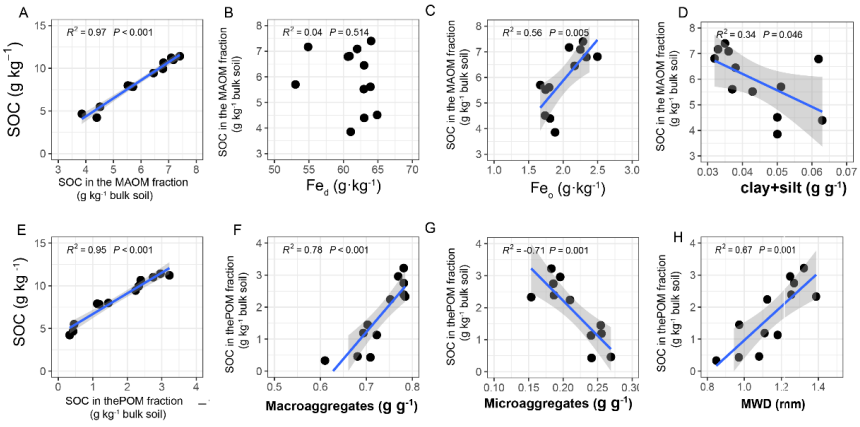

Fig. 3 The relationships between SOC and variables related to the chemical protection and physical protection. (A to D) Variables characterizing chemical protection, including the content of SOC stored in the MAOM fraction, the content of crystalline Fe oxides (Fe_d), the content of non-crystalline Fe oxides (Fe_o), and the content of clay and silt. (E to H) Variables characterizing physical protection, including the content of SOC stored in the POM fractions, the content of soil macroaggregates, the content of soil microaggregates and the mean weight diameter (MWD)

https://doi.org/10.5194/egusphere-2025-2405
Preprint. Discussion started: 25 June 2025

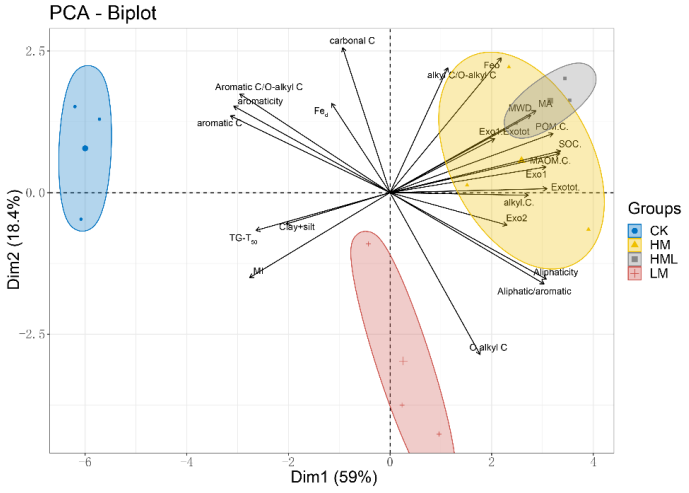

Fig. 4 Biplots of the principal component analysis (PCA) between the quantity and quality of SOC and variables related to chemical protection, physical protection across four manure application treatments (CK, Control; LM, low manure; HM, high manure; and HML, high manure plus lime). Fe_d, crystalline Fe oxides; Fe_o, non-crystalline Fe oxides; MA, macroaggregates (>0.25 mm); MI, microaggregates (0.05-0.25 mm); MWD, mean weight diameter; aromaticity, aromatic C / (alkyl C + O-alkyl C + aromatic C); aliphatic C, Alkyl C + O-alkyl C; aliphaticity, (Alkyl C + O-alkyl C) / (Alkyl C + O-alkyl C + Aromatic C); Exo_1, thermally labile soil organic matter (SOM); Exo_2, thermally stable SOM; Exo_{tot}, total SOM; TG-$T_{50,}$ the temperature at which half of the total SOM was lost

https://doi.org/10.5194/egusphere-2025-2405
Preprint. Discussion started: 25 June 2025

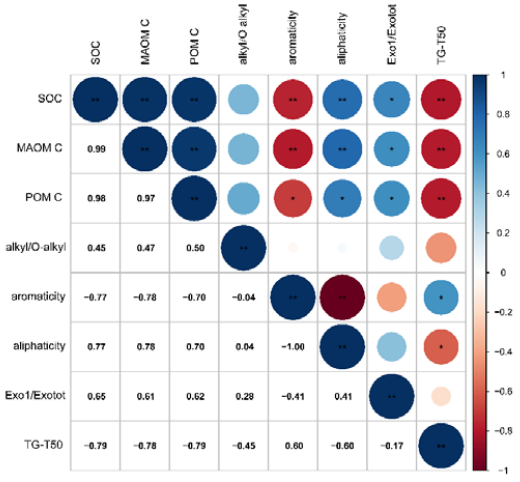

Fig. 5 The relationships between SOC quantity, chemical recalcitrance and thermal stability. Aromaticity, aromatic C / (alkyl C + O-alkyl C + aromatic C); aliphaticity, (alkyl C + O-alkyl C) / (alkyl C + O-alkyl C + aromatic C); Exo_1, thermally labile soil organic matter (SOM); Exo_{tot}, total SOM; $TG\text{-}T_{50,}$ the temperature at which half of the total SOM was lost